

Exhalation Spreading During Nasal High-Flow Therapy at Different Flow Rates

OBJECTIVES: Severe acute respiratory syndrome coronavirus 2 is transmitted through aerosols and droplets. Nasal high-flow therapy could possibly increase the spreading of exhalates from patients. The aim of this study is to investigate whether nasal high-flow therapy affects the range of the expiratory plume compared with spontaneous breathing.

DESIGN: Interventional experiment on single breaths of a healthy volunteer.

SETTING: Research laboratory at the Bauhaus-University Weimar.

SUBJECTS: A male subject.

INTERVENTIONS: Videos and images from a schlieren optical system were analyzed during spontaneous breathing and different nasal high-flow rates.

MEASUREMENTS AND MAIN RESULTS: The maximal exhalation spread was 0.99, 2.18, 2.92, and 4.1 m during spontaneous breathing, nasal high-flow of 20L/min, nasal high-flow of 40L/min, and nasal high-flow of 60L/min, respectively. Spreading of the expiratory plume in the sagittal plane can completely be blocked with a surgical mask.

CONCLUSIONS: Nasal high-flow therapy increases the range of the expiratory air up to more than 4 meters. The risk to pick up infectious particles could be increased within this range. Attachment of a surgical mask over the nasal high-flow cannula blocks the expiratory airstream.

KEY WORDS: infection control; nasal high-flow; respiratory failure; respiratory support; schlieren imaging; severe acute respiratory syndrome coronavirus 2

Dominic Dellweg, PhD^{1,2}

Jens Kerl, PhD^{1,2}

Amayu Wakoya Gena, MArch³

Hayder Alsaad, PhD³

Conrad Voelker, PhD³

Severe acute respiratory syndrome coronavirus 2 (SARS-CoV-2) infections have rapidly increased in numbers since the association between the virus and the clinical picture of coronavirus disease 2019 (COVID-19) which were recognized in December 2019 (1). First world countries were facing resource scarcity for patients with SARS-CoV-2 associated respiratory failure (2). There is an ongoing debate about the mode of transmission of SARS-CoV-2 virus. The World Health Organization is currently starting from the premise that COVID-19 is being transmitted mainly by droplets of different sizes and that transmission of the virus occurs within a range of 1 meter surrounding the source of infection (3). Thus, a safety clearance of 1.5 to 2 meters or 6 feet would be sufficient to prevent viral transmission and infection (3, 4). Hanging aerosols, however, have recently been addressed as a major route in the transmission process (5). Recent studies suggest that transmission of at least 1,000 viral copies is required to cause an infection (6).

Nasal high-flow (NHF) therapy has been shown to improve outcomes in hypoxemic respiratory failure (7) and has been used by different groups during

Copyright © 2021 The Author(s). Published by Wolters Kluwer Health, Inc. on behalf of the Society of Critical Care Medicine and Wolters Kluwer Health, Inc. This is an open-access article distributed under the terms of the Creative Commons Attribution-Non Commercial-No Derivatives License 4.0 (CCBY-NC-ND), where it is permissible to download and share the work provided it is properly cited. The work cannot be changed in any way or used commercially without permission from the journal.

DOI: 10.1097/CCM.0000000000005009

the SARS-CoV-2 pandemic (8, 9). The use of NHF is recommended by different societies and expert groups (10–15). Although data suggest that NHF does not pose an increased risk for the spread of bacteria (16), there is a growing concern that NHF is a risk factor for viral transmission through aerosols (17, 18). Hui et al (19) examined the effect of NHF on the expiratory plume with a human patient simulator by means of smoke particles and laser light visualization. The exhaled aerosol expansion was less than 62 cm at a high-flow rate of 60 L/min indicating that a safety distance of 1.5 to 2 m is adequate (19). Gaeckle et al (20) published an investigation indicating no increase in aerosol generation during NHF therapy using a funnel sampler and a particle detector five cm away from the patient's face. A recent publication has, however, demonstrated that expiratory plumes induced by sneezing can reach distances of up to 8 meters (21). Therefore, researchers from China recommend applying surgical masks to patients during NHF therapy (22). Nevertheless, the impact of NHF on expiratory airflow formation and distribution has never been evaluated using human subjects. To visualize and evaluate this distribution, schlieren optical measurement can be applied. It is a noninvasive procedure to visualize exhaled plumes and airflows from human patient simulators (23) as well as human beings (24). The rationale of this investigation is to describe and quantify the expiratory plumes during spontaneous breathing as well as during the application of NHF at different flow rates with and without the attachment of surgical masks during NHF therapy.

METHODS

Schlieren Imaging System

The experiments were conducted using an optical schlieren imaging system at the Bauhaus-University Weimar. The schlieren technique allows visualizing density gradients of fluids by capitalizing the refraction of light when entering a medium of different density. As illustrated in **Figure 1**, the implemented schlieren system consists of a single concave spherical mirror, a light source, a knife-edge schlieren cutoff, and a digital camera. The used schlieren mirror has an astronomical quality with a surface accuracy of $\lambda/9.75$, where λ is the wavelength of helium-neon laser light in nm. Such accuracy is necessary to allow visualizing weak indoor airflows that refract the light by less

than 1 arcsecond. With a diameter of 1 m, the mirror is among the largest schlieren mirrors in the world. The mirror is made from Astrosital glass-ceramic with a thickness-to-diameter ratio of 0.11. It has a 2.7 nm root mean square micro-roughness and a scratch/dig surface quality of 100/80. The schlieren imaging system is situated in a laboratory hall with the dimensions of $11.72 \times 6.44 \times 2.80$ m. The light source is placed on the axis of the spherical mirror at its radius of curvature ($R = 6,003$ mm). The light source in this system is a small light-emitting diode with $2.1 \times 2.1 \times 0.27$ mm size, 284 lm luminous flux, and 5000 K color temperature. To capture the schlieren images, a high-resolution Canon EOS 5DS R camera with 50.6 megapixels image size and a 135 mm focal-length lens was used. The camera was set manually to a shutter speed of 1/60 s, International Organisation for Standardization 320, a lens aperture of F2.0, and an image resolution of $1,280 \times 720$ pixels. These settings were chosen to obtain high-quality single images with a correct exposure at a low light level in the room. For visualization of air movement, the schlieren videos were recorded at 50 frames/s. Detailed physical properties as well as the mathematical model of the schlieren system can be found in our previously published work (23, 25).

Experimental Setup

The study was conducted using a human test subject seated in front of the mirror and equipped with an NHF therapy device (**Fig. 2**). The study was approved by the responsible authority (AEKWL 2020-659-f-S). In the present study, the NHF system (Airvo-2; Fisher & Paykel, Auckland, New Zealand) was used with a medium-size NHF-cannula (Optiflow; Fisher & Paykel). The water chamber of the device was filled according to the manufacturer's specifications. The device temperature was set to 37°C; the device delivers air with a relative humidity of 100% via heated tubing to prevent water condensation. Thus, exhaled air from the test subject and air from the high-flow device had similar physical properties, which are of importance since heat and humid air may influence the index of refraction visualized by the schlieren technique. The distance between the mirror and the center of the subject's head was 80 cm. The test subject was a healthy 33 years old male person, 177 cm in height with a body mass index of 20.4 kg/m². To prevent the convective

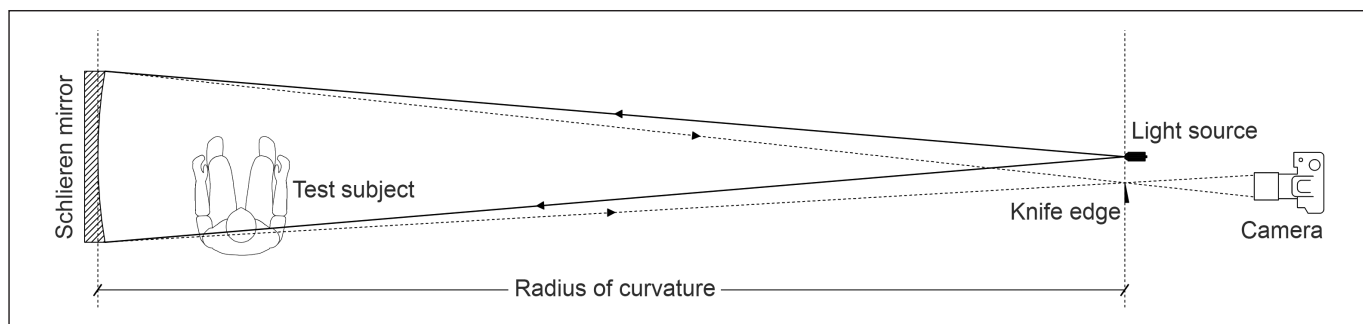


Figure 1. The setup scheme of the schlieren imaging system (*top view*).

flow above the thighs from interfering with the visualized exhaled air, a cardboard sheet was placed against the subject's abdomen at 8 cm above the thighs to block the ascending flow. Additionally, the test subject was wearing loose winter attire, which reduced the velocity of the convective flow in the vicinity of the body (26). This diminished its impact on the visualized exhaled flow.

The subject's respiration was monitored with a standard sleep laboratory polygraphic system (SOMNOscreen plus recorder system; SOMNOmedics,

Randersacker, Germany). This was necessary to ensure equal tidal volumes throughout the experiment. The respiratory inductance plethysmography (RIP) belts were placed around the chest and abdomen of the subject. The RIP signals were calibrated using the somnomedics pneumotachograph prior to each test run. Polygraphic recordings were transmitted via wireless local area network to a receiver connected to a standard laptop computer, on which the recording/analyzing software of the polygraphic system was installed (DOMINO Software package; SOMNOmedics). This setup allowed a retrospective video-synchronized breath-by-breath analysis of airflow and expiratory tidal volume with a time resolution/sampling rate of 32 Hz.

Three NHF flow rates were tested: 20, 40, and 60 L/min in addition to a reference case with spontaneous (unassisted) breathing. Furthermore, additional tests were conducted with NHF in combination with a standard surgical mask covering the subject's nose and mouth. For each test run, a 2-minute video was recorded resulting in 6,000 frames for each setup. Both lateral as well as anterior-posterior positions related to the plane of the schlieren mirror were investigated.

Image Analysis

As the visualization of the expiratory plume is limited to the 1-meter diameter of the schlieren mirror, the captured schlieren images were analyzed to forecast the airflow outside the range of the optical system. The decrease of the horizontal velocity component of the exhaled airstream was extrapolated down to complete stasis, which provided the sought information about the range of the expiratory plume. This was achieved by exporting the captured 2-minute videos consisting of 6,000 single frames each using MATLAB (The MathWorks, Inc., Natick, MA). For each NHF volume,

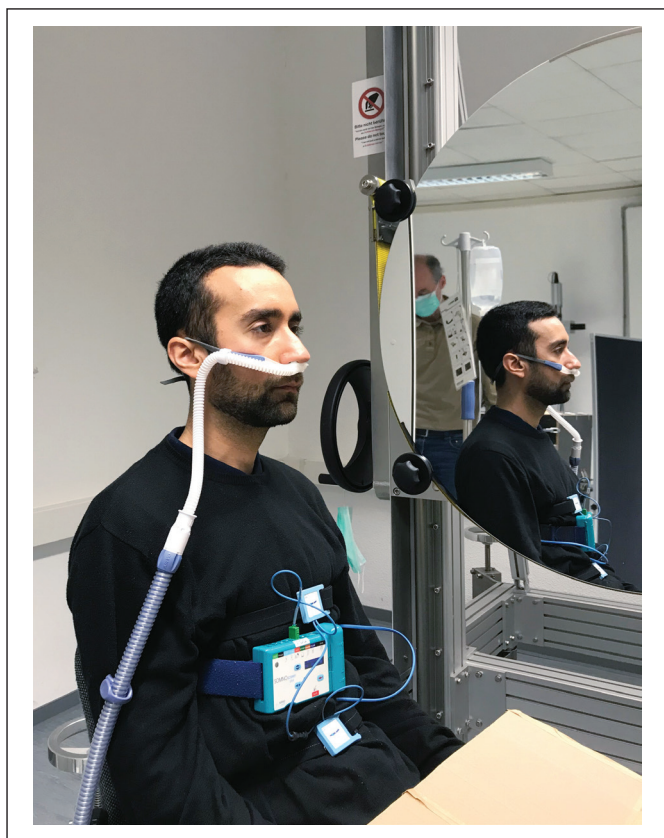


Figure 2. One of the authors served as the test subject. He is seated in front of the schlieren mirror wearing the nasal high-flow therapy device.

fully developed exhaled plumes that were generated at similar tidal volume were selected for analysis. The selection of these exhalations was not randomly, as only fully developed exhaled plumes were chosen. This made sure to analyze the ones with the farthest reach. Still, it took plenty of time and effort to analyze dozens of pictures for each single exhalation, as this needed to be done manually. The selected frames were imported into AutoCAD (Autodesk, San Rafael, CA) to measure the spread distance from the mouth to the wave-front of the expired air for each frame. Subsequently, the horizontal velocity component was calculated based on the traveled distance and the time taken by the wave-front to travel that distance. By dint of linear regression, the air velocity was extrapolated down to complete stasis to calculate the final spread distance of the exhaled air for each NHF volume.

Additionally, the PIVlab (<https://pivlab.blogspot.com>) cross-correlation algorithm (27) was used in MATLAB to generate the velocity colormaps. A full description of the generation approach can be found in Gena et al (23). These colormaps were produced to qualitatively illustrate the spread velocity of the exhaled air from the test subject.

RESULTS

Supplemental Figure 1 (<http://links.lww.com/CCM/G326>; **legend**, <http://links.lww.com/CCM/G334>) shows static images of the expiratory plume within the range of the 1 m diameter of the schlieren mirror during spontaneous breathing as well as NHF application at 20, 40, and 60 L/min. The schlieren images show a clear increase in the spread of exhaled air when NHF is used compared with the reference case of spontaneous breathing. The velocity colormaps indicate an increase in exhaled velocity and a change in the inclination of the exhaled jet when increasing the flow rate of NHF. When a standard surgical mask is used with NHF therapy, the exhaled airstream was remarkably blocked and mixed with the ascending convective flow. This can be seen in the schlieren images as well as in the velocity colormaps. For a better demonstration of the exhaled plumes, the captured schlieren videos are enclosed with the article (**Supplemental Video 1**, <http://links.lww.com/CCM/G327>; **Supplemental Video 2**, <http://links.lww.com/CCM/G328>; **Supplemental Video 3**, <http://links.lww.com/CCM/G329>;

Supplemental Video 4, <http://links.lww.com/CCM/G330>; **Supplemental Video 5**, <http://links.lww.com/CCM/G331>; **Supplemental Video 6**, <http://links.lww.com/CCM/G332>; and **Supplemental Video 7**, <http://links.lww.com/CCM/G333> [legend, <http://links.lww.com/CCM/G334>]).

Among the multiple analyzed exhaled plumes, **Figure 3** presents the exhalation velocity of a selected exhaled plume within the range of the schlieren mirror. The presented plumes in **Figure 3** were selected as they had the longest spreading distance and comparable tidal volumes at the same time (756 ± 9 mL [range, 747–766 mL]). As the exhaling mouth was not completely at the edge of the mirror (**Supplemental Fig. 1**, <http://links.lww.com/CCM/G326>; legend, <http://links.lww.com/CCM/G334>), the end of the mirror was reached after 0.6–0.7 m. Since the use of a surgical mask blocked the exhaled flow, there was no wave-front for quantitative evaluation. Therefore, the cases of NHF + mask are not included in **Figure 3**.

From the video material, the static images in **Supplemental Figure 1** (<http://links.lww.com/CCM/G326>; legend, <http://links.lww.com/CCM/G334>), and the diagrams in **Figure 3**, it becomes obvious that the expiratory plume without the surgical mask exceeds the area of the schlieren mirror. According to **Figure 3**, linear deceleration of airstream velocity was the best fit for the function velocity versus distance. The extrapolation of data beyond 1 m is shown in **Figure 4**, where maximal distance is reached at zero horizontal airstream velocity. The maximal exhalation spread was 0.99, 2.18, 2.92, and 4.1 m during spontaneous breathing, NHF 20 L/min, NHF 40 L/min, and NHF 60 L/min, respectively. Anterior-posterior imaging did not show any recognizable change in the expiratory plume in between the four different test runs and did not differ from the thermal plume seen during breath holding.

DISCUSSION

Our data suggest that the expiratory plume extends much further than previously suspected (19). During NHF treatment, a 2-meter safety clearance would already be insufficient at a flow rate of 20 L/min. Sixty liters of NHF per minute would already require a safety distance of more than 4 meters. Expiratory plumes spread away from the patient's face along a sagittal plane in relatively narrow sectors as shown in

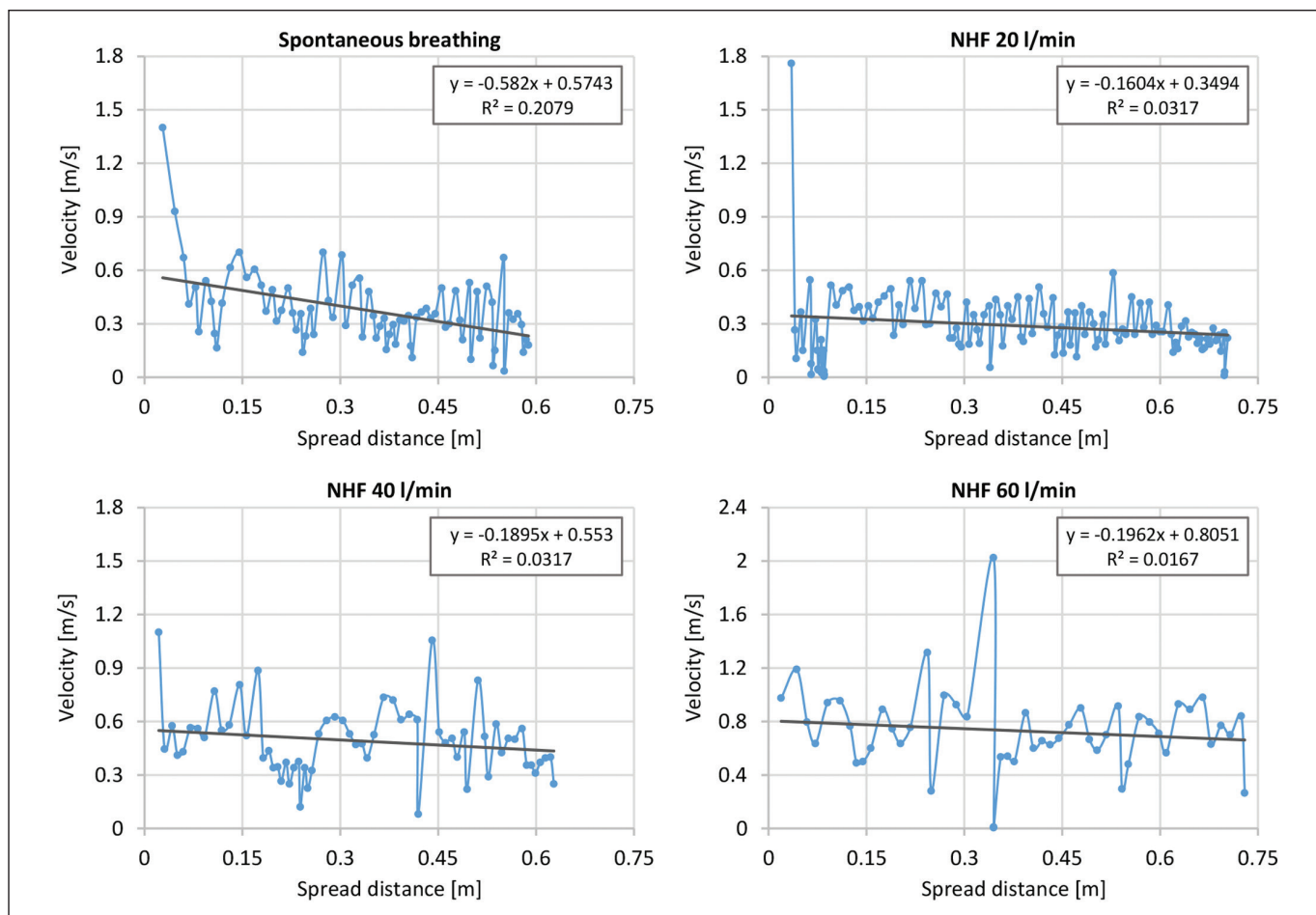


Figure 3. Exhaled flow velocity within the range of the schlieren mirror when the surgical mask was not used with nasal high-flow (NHF).

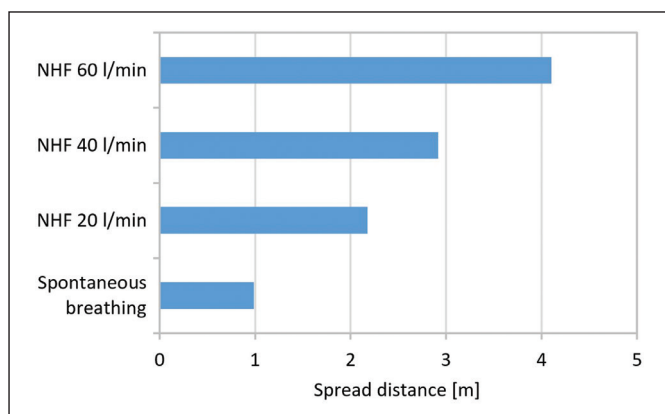


Figure 4. The calculated spread distance of nasal high-flow without surgical masks.

Supplemental Figure 1 (<http://links.lww.com/CCM/G326>; legend, <http://links.lww.com/CCM/G334>). Any change in head position, however, will change the direction of the expiratory plume accordingly. This will make the safety area around an infected person highly variable.

These results differ from those reported in Hui et al (19), which could not detect any particles beyond 62 cm distance from the dummy's face at NHF flow rates of 60 L/min using 1- μ m oil-based smoke particles. Schlieren imaging, on the other hand, visualizes the expired airflow; this technique is highly unlikely to overestimate true airstreams. The linear function in velocity deceleration allows a quite exact determination of the expiratory plume range.

NHF has been shown to reduce the work of breathing. This is due to the washout effect as well as to the positive airway pressure that is generated through the flow (28–31). In patients with lung disease, this might decrease tidal volumes with increasing NHF flow rates (32, 28). Our experimental setup did not take that into account since we wanted to show the isolated effect of NHF flow rate on the dimensions of the expiratory plume. Since tidal volumes were almost identical throughout the measurements, the increase in plume dimensions must be a function of NHF flow rate.

Expiratory aerosols develop during inspiration in the distal airways of the lungs; the amount of aerosol particles expelled during expiration correlates with the depth of the foregone inspiration (33). The spectrum of aerosol diameter during expiration is broad and ranges between 0.05 and 5 μm during normal breathing (33). Activities such as talking or coughing already generate particles with a mass median aerodynamic diameter of 13.5 and 16 μm , respectively (34). Assuming an equal specific weight of particles, a 5 μm measuring particle has, for example, a 125-fold volume and mass of a 1 μm measuring particle (35) since volume goes along with the third decimal potency of the radius. The kinetic energy of any particles is determined by particle mass and the square of the particle velocity. In addition, particles undergo a shrinking process and lose mass due to evaporation when they leave the humid environment of the human body (35, 36). These physical principles illustrate the complexity of aerosol movements in expiratory plumes. An in-depth illustration of complex mathematical models to determine movements of single particles is beyond the scope of this article and can be found in dedicated papers (36).

Schlieren imaging technique visualizes density gradients of fluids, in this case of the expiratory plume. It does not provide information about particle concentration, nor does it allow a characterization of particle size distribution within the expiratory plume. Particles measuring 5 μm have a sedimentation rate of only 0.74 mm/s and can remain airborne for a long time (35). Particles smaller than 0.5 to 1 μm can remain airborne indefinitely (35, 37). According to Figure 4 and Supplemental Figure 1 (<http://links.lww.com/CCM/G326>; legend, <http://links.lww.com/CCM/G334>), particles have a transit time of about 6 seconds allowing for a relevant change in particle size reduction due to evaporation (35, 36). A recent investigation showed that SARS-CoV-2 virus can remain vital and airborne in aerosols for at least 3 hours (38). Previous publications have shown that NHF reduces particle concentration at 5 cm (20) and at one foot and three feet (30.48 and 91.44 cm) (39) away from the patient's head. This can potentially be explained by the diluting effect of air coming from the NHF system. When the patient's particle-rich air mixes with the low-particle air from the NHF system in the upper respiratory tract, it is expelled as a mixture with a lower particle concentration but a greater range according to our results. In patients with lung disease, however, NHF has

been shown to reduce the work of breathing and minute ventilation (32, 28). Since particle generation correlates to the depth of breathing, NHF therapy could even reduce the total exhaled particle load. Since more and more authors propagate an airborne transmission mode for the SARS-CoV-2 virus (5, 40–42), there is an urgent need to classify particle size distribution in expiratory plumes during NHF treatment as a function of the distance to the patient's head. Until then, it can be assumed that a further spread of particles is within the ranges we have described and that particle concentration is likely to be homogeneously distributed in the patient's room. Epidemiological studies have shown that the risk of infection is linked to measures that are carried out in the proximity of the patient (43). NHF might change this risk stratification. Another important aspect is the displacement of air after several consecutive breaths. Given the same head position and direction of the expiratory airstream, every new expiratory plume displaces air of the previous exhalation and potentially pushes infective aerosols that have not deposited further away from the patient into the room. This mechanism might spread infective particles much further than previously thought.

There was no detectable expiratory plume in the sagittal plane when the test subject wore a surgical mask. This approach was suggested in a report from China (22). Furthermore, a recent report using computational fluid dynamics simulations published results that agree with our findings (44). However, the feasibility of this approach has not been investigated on human beings. In Theory, airstream interference with the surgical mask could compromise the washout effect of NHF. More research is needed to answer this question. Until then, careful monitoring is warranted for patients wearing masks during NHF.

LIMITATIONS

Evidence suggests that at least during invasive ventilation, the addition of end-expiratory pressure increases the emission of the virus from the lungs (45). Bräunlich et al (30) pointed out that NHF has a washout effect that can even be measured in the distal airways. Furthermore, they described a flow-dependent positive pressure effect in the distal airways of the lungs. More research is needed to investigate whether NHF only increases the dimensions of the expiratory plume and thereby dilutes the viral concentration or whether

NHF increases the absolute amount of virus expelled from the lungs. We conducted our measurements on single breaths of a healthy human subject. However, we kept the tidal volume constant during the experiments as described in the method section, and we would expect to observe similar results if more subjects would have been included.

CONCLUSIONS

The range of the expiratory plume of a single breath, measured in a healthy person, increases with increasing NHF flow rates with a maximum of 4.1 m during NHF treatment with 60 L/min. Thus, expiratory air during NHF travels further than previously suggested and infectious aerosols might spread faster than during unassisted breathing. Wearing a surgical mask over the NHF prongs blocks the expiratory plume during all NHF flow rates. Whether the latter approach compromises, NHF efficacy has not been investigated to date.

1 Department for Pulmonary and Intensive Care Medicine, Kloster Grafschaft, Schmallingenberg, Germany.

2 Departement for Medicine, Philipps University Marburg, Marburg, Germany.

3 Department of Building Physics, Bauhaus-University Weimar, Weimar, Germany.

Supplemental digital content is available for this article. Direct URL citations appear in the printed text and are provided in the HTML and PDF versions of this article on the journal's website (<http://journals.lww.com/ccmjjournal>).

Drs. Dellweg and Voelker designed the study. Dr. Kerl, Mr. Gena, and Dr. Alsaad conducted the experiments. Gena and Dr. Voelker analyzed the data acquired from the optical system. Dr. Kerl analyzed the data from the polygraphic system. Dr. Dellweg drafted the article. Drs. Alsaad and Voelker reviewed and edited the article. All authors have read the article and agree with the content. Dr. Kerl received funding from ResMed Healthcare. The remaining authors have disclosed that they do not have any potential conflicts of interest.

For information regarding this article, E-mail: d.dellweg@fkk.de

REFERENCES

- Zhu N, Zhang D, Wang W, et al: A novel coronavirus from patients with pneumonia in China, 2019. *N Engl J Med* 2020; 382:727–733
- White DB, Lo B: A framework for rationing ventilators and critical care beds during the COVID-19 pandemic. *J Am Med Assoc* 2020; 323:1773–1774
- World Health Organization: Modes of Transmission of Virus Causing COVID-19: Implications for IPC Precaution Recommendations. Geneva, Switzerland, World Health Organization, 2020. Available at: <https://www.who.int/news-room/commentaries/detail/modes-of-transmission-of-virus-causing-covid-19-implications-for-ipc-precaution-recommendations>. Accessed December 30, 2020
- Centers for Disease Control and Prevention: What Is Social Distancing? Atlanta, GA, Centers for Disease Control and Prevention, 2020. Available at: <https://www.cdc.gov/coronavirus/2019-ncov/prevent-getting-sick/social-distancing.html>. Accessed December 30, 2020
- Scheuch G: Breathing is enough: For the spread of influenza virus and SARS-CoV-2 by breathing only. *J Aerosol Med Pulm Drug Deliv* 2020; 33:230–234
- Popa A, Genger J-W, Nicholson M, et al: Genomic epidemiology of superspreading events in Austria reveals mutational dynamics and transmission properties of SARS-CoV-2. *Sci Transl Med* 2020; 12:eabe2555
- Frat J-P, Thille AW, Mercat A, et al: High-flow oxygen through nasal cannula in acute hypoxemic respiratory failure. *N Engl J Med* 2015; 372:2185–2196
- Wang D, Hu B, Hu C, et al: Clinical characteristics of 138 hospitalized patients with 2019 novel coronavirus-infected pneumonia in Wuhan, China. *J Am Med Assoc* 2020; 323:1061–1069
- Chen Q, Zheng Z, Zhang C, et al: Clinical characteristics of 145 patients with corona virus disease 2019 (COVID-19) in Taizhou, Zhejiang, China. *Infection* 2020; 48:543–551
- Italian Thoracic Society: Managing the Respiratory Care of Patients With COVID-19. Available at: <https://ers.app.box.com/s/j09ysr2kdhmkc1ulm8y8dxnosm6yi0h>. Accessed December 30, 2020
- Chu DK, Akl EA, Duda S, et al: Physical distancing, face masks, and eye protection to prevent person-to-person transmission of SARS-CoV-2 and COVID-19: A systematic review and meta-analysis. *Lancet* 2020; 395:1973–1987
- Australian and New Zealand Intensive Care Society: COVID-19 Guidelines. 2020. Available at: https://www.anzics.com.au/wp-content/uploads/2020/10/ANZICS-COVID-19-Guidelines_V3.pdf. Accessed December 7, 2020
- National Institutes of Health: COVID-19 Treatment Guidelines. 2020. Available at: <https://www.covid19treatmentguidelines.nih.gov/critical-care/oxygenation-and-ventilation/>. Accessed July 17, 2020
- Alhazzani W, Møller MH, Arabi YM, et al: Surviving Sepsis Campaign: Guidelines on the management of critically ill adults with coronavirus disease 2019 (COVID-19). *Intensive Care Med* 2020; 46:854–887
- Pfeifer M, Ewig S, Voshaar T, et al: Position paper for the state-of-the-art application of respiratory support in patients with COVID-19. *Respiration* 2020; 99:521–542
- Leung CCH, Joynt GM, Gomersall CD, et al: Comparison of high-flow nasal cannula versus oxygen face mask for

- environmental bacterial contamination in critically ill pneumonia patients: A randomized controlled crossover trial. *J Hosp Infect* 2019; 101:84–87
17. Remy KE, Lin JC, Verhoef PA: High-flow nasal cannula may be no safer than non-invasive positive pressure ventilation for COVID-19 patients. *Crit Care* 2020; 24:169
 18. National Health Service: Guidance for the Role and Use of Non-Invasive Respiratory Support in Adult Patients With Coronavirus (Confirmed or Suspected). 2020. Available at: <https://amhp.org.uk/app/uploads/2020/03/Guidance-Respiratory-Support.pdf>. Accessed December 6, 2020
 19. Hui DS, Chow BK, Lo T, et al: Exhaled air dispersion during high-flow nasal cannula therapy versus CPAP via different masks. *Eur Respir J* 2019; 53:1802339
 20. Gaeckle NT, Lee J, Park Y, et al: Aerosol generation from the respiratory tract with various modes of oxygen delivery. *Am J Respir Crit Care Med* 2020; 202:1115–1124
 21. Bourouiba L: Turbulent gas clouds and respiratory pathogen emissions: Potential implications for reducing transmission of COVID-19. *JAMA* 2020; 323:1837–1838
 22. He G, Han Y, Fang Q, et al: Clinical experience of high-flow nasal cannula oxygen therapy in severe COVID-19 patients. *Zhejiang Da Xue Xue Bao Yi Xue Ban* 2020; 49:232–239
 23. Gena AW, Voelker C, Settles GS: Qualitative and quantitative schlieren optical measurement of the human thermal plume. *Indoor Air* 2020; 30:757–766
 24. Tang JW, Liebner TJ, Craven BA, et al: A schlieren optical study of the human cough with and without wearing masks for aerosol infection control. *J R Soc Interface* 2009; 6(Suppl 6):S727–S736
 25. Alsaad H, Voelker C: Qualitative evaluation of the flow supplied by personalized ventilation using schlieren imaging and thermography. *Build Environ* 2020; 167:106450
 26. Licina D, Pantelic J, Melikov A, et al: Experimental investigation of the human convective boundary layer in a quiescent indoor environment. *Build Environ* 2014; 75:79–91
 27. Thielicke W, Stamhuis EJ: PIVlab – towards user-friendly, affordable and accurate digital particle image velocimetry in MATLAB. *J Open Res Softw* 2014; 2:e30
 28. Mauri T, Turrini C, Eronia N, et al: Physiologic effects of high-flow nasal cannula in acute hypoxemic respiratory failure. *Am J Respir Crit Care Med* 2017; 195:1207–1215
 29. Möller W, Feng S, Domanski U, et al: Nasal high flow reduces dead space. *J Appl Physiol* 2017; 122:191–197
 30. Bräunlich J, Goldner F, Wirtz H: Nasal highflow eliminates CO₂ from lower airways. *Respir Physiol Neurobiol* 2017; 242:86–88
 31. Bräunlich J, Köhler M, Wirtz H: Nasal highflow improves ventilation in patients with COPD. *Int J COPD* 2016; 11:1077–1085
 32. Delorme M, Bouchard PA, Simon M, et al: Effects of high-flow nasal cannula on the work of breathing in patients recovering from acute respiratory failure. *Crit Care Med* 2017; 45:1981–1988
 33. Schwarz K, Biller H, Windt H, et al: Characterization of exhaled particles from the healthy human lung—a systematic analysis in relation to pulmonary function variables. *J Aerosol Med Pulm Drug Deliv* 2010; 23:371–379
 34. Chao CYH, Wan MP, Morawska L, et al: Characterization of expiration air jets and droplet size distributions immediately at the mouth opening. *J Aerosol Sci* 2009; 40:122–133
 35. Köhler D, Fleischer W: Inhalationstherapie. München, Germany, Arcis Verlag, 2000
 36. Xie X, Li Y, Chwang ATY, et al: How far droplets can move in indoor environments - revisiting the Wells evaporation-falling curve. *Indoor Air* 2007; 17:211–225
 37. Brain JD, Valberg PA: Deposition of aerosol in the respiratory tract. *Am Rev Respir Dis* 1979; 120:1325–1373
 38. van Doremalen N, Bushmaker T, Morris DH, et al: Aerosol and surface stability of SARS-CoV-2 as compared with SARS-CoV-1. *N Engl J Med* 2020; 382:1564–1567
 39. Li J, Fink JB, Elshafei AA, et al: Placing a mask on COVID-19 patients during high-flow nasal cannula therapy reduces aerosol particle dispersion. *ERJ Open Res* 2020; 7:00519–2020
 40. Prateek B, Doolan C, de Silva C, et al: Airborne or droplet precautions for health workers treating COVID-19? *J Infect Dis* 2020 Apr 16. [online ahead of print]
 41. Setti L, Passarini F, De Gennaro G, et al: Airborne transmission route of covid-19: Why 2 meters/6 feet of inter-personal distance could not be enough. *Int J Environ Res Public Health* 2020; 17:2932
 42. Morawska L, Cao J: Airborne transmission of SARS-CoV-2: The world should face the reality. *Environ Int* 2020; 139:105730
 43. Raboud J, Shigayeva A, McGeer A, et al: Risk factors for SARS transmission from patients requiring intubation: A multicentre investigation in Toronto, Canada. *PLoS One* 2010; 5:e10717
 44. Leonard S, Atwood CW Jr, Walsh BK, et al: Preliminary findings on control of dispersion of aerosols and droplets during high-velocity nasal insufflation therapy using a simple surgical mask: Implications for the high-flow nasal cannula. *Chest* 2020; 158:1046–1049
 45. Wan GH, Wu CL, Chen YF, et al: Particle size concentration distribution and influences on exhaled breath particles in mechanically ventilated patients. *PLoS One* 2014; 9:e87088